Dalton Transactions

PAPER

View Article Online
View Journal | View Issue

Cite this: *Dalton Trans.*, 2014, **43**, 1125

Synthesis, structure and photophysical properties of $[UO_2X_2(O{=}PPh_3)_2]$ (X = Cl, Br, I)†

Emtithal Hashem,[a] Thomas McCabe,[a] Carola Schulzke[b] and Robert J. Baker*[a]

Received 10th September 2013,
Accepted 23rd October 2013

DOI: 10.1039/c3dt52480a

www.rsc.org/dalton

The synthesis of a series of uranyl compounds *via* oxidation of $[Li(THF)_4][UX_5(THF)]$ (X = Cl, Br, I) in the presence of $Ph_3P{=}O$ is described. The solid state structures of $[Li(O{=}PPh_3)(MeCN)_2]_2[UO_2Cl_4]$, $[UO_2Br_2(O{=}PPh_3)_2]$ and $[Li(O{=}PPh_3)_4][I_3]$, formed as a by-product from the oxidation of $[Li(THF)_4][UI_5(THF)]$, is reported. The electronic absorption spectra and photoluminescence spectra of $[UO_2X_2(O{=}PPh_3)_2]$ (X = Cl, Br, I) have been measured and no significant changes in the position of the emission (515–530 nm) or the lifetimes (*ca.* 1 μs) are observed in this series. However a bathochromic shift is observed in the U–X LMCT band in the electronic absorption spectrum.

Introduction

The chemistry of the actinides has undergone a resurgence of interest over the past decade, with small molecule activation at the forefront of this revolution.[1] Reactivity patterns have been developed that have no analogue in transition metal chemistry.[2] This has fuelled a deeper understanding of the bonding in these compounds, particularly the role the 5f and 6d orbitals play in metal–ligand interactions.[3] One class of compounds that has known covalency is the uranyl ion, $\{UO_2\}^{2+}$.[4] However, it has taken some time to fully elucidate the bonding in this species, which has immense importance as it is in the most stable oxidation state and prevalent in the environment and in spent nuclear fuels. A comprehensive understanding has come from both experiment and theory and an authoritative review by Denning summarises recent developments.[5] Detailed studies of $[UO_2Cl_4]^{2-}$ have substantially aided in the description of the bonding in the uranyl fragment. The photophysical properties of the uranyl ion have been elucidated from these studies and the optical properties are due to a ligand-to-metal charge transfer (LMCT) transition involving promotion of an electron from a bonding –yl oxygen orbital (σ_u, σ_g, π_u and π_g) to a non-bonding uranium $5f_\delta$ and $5f_\phi$ orbital, centred at *ca.* 420 nm. The characteristic green emission arises from de-excitation of this $^3\Pi_u$ triplet excited state. Superimposed on the absorption and emission bands are 'hot bands' arising from strong coupling of the ground state Raman active symmetric vibrational O=U=O (ν_1) mode with the $^3\Pi_u$ electronic triplet excited state. The heavier halides have been less well studied with few examples of structurally characterised $[UO_2Br_4]^{2-}$.[6] Due to the decrease in the U–X bond energy, which has been documented for UX_3 (U–F = 619 kJ mol^{-1}, U–Cl = 495.4 kJ mol^{-1}, U–Br = 424.3 kJ mol^{-1}, and U–I = 343 kJ mol^{-1}),[7] uranyl iodides are rare. The first example unambiguously reported was the thermally unstable $[UO_2I_2(H_2O)_2]{\cdot}4Et_2O$,[8] but since then further thermally stable compounds have been prepared, such as $[UO_2I_2(py)_3]$,[9] $[UO_2I_2L_2]$ (L = $O{=}PPh_3$, $O{=}P(NMe_2)_3$)[7] and $[Ph_4P]_2[UO_2I_4]$.[10] The bonding in $[UO_2X_2(O{=}PPh_3)_2]$ has been explored computationally and found that as the size of the halogen increases, the covalent interactions between U and X increases.[11] To the best of our knowledge, the emissive properties of these heavier halides have not been reported in fluid solution.

We have an interest in uranyl chemistry and have recently reported upon the use of neutral uranyl halides and uranyl aryloxides as catalysts for the ring opening polymerisation of epoxides and lactones.[12] We also recently discussed the photoluminescence properties of simple U(IV) compounds which was observed for the first time in non-aqueous media.[13] We have begun to explore the synthetic utility of $[Li(THF)_4][UX_5(THF)]$ (X = Cl, Br, I) and herein we report on the oxidation of these species in the presence of $Ph_3P{=}O$. A comparison of the absorption and photoluminescence spectra on the series of compounds $[UO_2X_2(O{=}PPh_3)_2]$ (X = Cl, Br, I) will be discussed.

Results and discussion

We recently showed that exposure of $[Li(THF)_4][UCl_5(THF)]$ to air in pyridine formed the uranyl complex $[PyH]_2[UO_2Cl_4]$ in

[a]*School of Chemistry, University of Dublin, Trinity College, Dublin 2, Ireland. E-mail: bakerrj@tcd.ie; Fax: +353(0)1 6712826; Tel: +353-(0)1-8963501*
[b]*Institut für Biochemie, Ernst-Moritz-Arndt Universität Greifswald, Felix-Hausdorff-Straße 4, D-17487 Greifswald, Germany*

†Electronic supplementary information (ESI) available: UV-vis spectra and vibrational data of **1**, **3** and **4**. CCDC 959953–959955. For ESI and crystallographic data in CIF or other electronic format see DOI: 10.1039/c3dt52480a

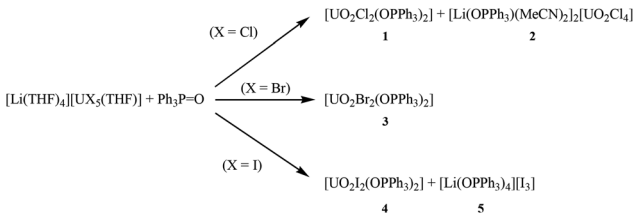

Scheme 1

good yield.[13] Given that we had in hand the analogous $[Li(THF)_4][UX_5(THF)]$ (X = Br, I) we sought to extend the reactivity to prepare stable uranyl halide compounds and thus explore the photoluminescence properties of a series of uranyl compounds where the halide is systematically varied. We found that addition of $Ph_3P{=}O$ to the U(IV) species before air oxidation afforded a suitable route to these species. Upon addition of a THF solution of $Ph_3P{=}O$ to the U(IV) compound followed by exposure to air, a colour change to yellow was observed which indicates the formation of a uranyl moiety (Scheme 1). The products of this reaction depended upon the halide. When X = Cl two products were obtained that could be separated by fractional recrystallisation. The major product was the known compound $[UO_2Cl_2(O{=}PPh_3)_2]$, **1**,[14] whilst ~10% was $[Li(O{=}PPh_3)(MeCN)_2]_2[UO_2Cl_4]$, **2**. When X = Br the compound $[UO_2Br_2(O{=}PPh_3)_2]$, **3**, was exclusively formed, whilst when X = I $[UO_2I_2(O{=}PPh_3)_2]$, **4**, was obtained, along with $[Li(O{=}PPh_3)_4][I_3]$, **5**, which could be readily separated by hand. We have been unable to grow crystals of $[UO_2I_2(O{=}PPh_3)_2]$[7] suitable for X-ray diffraction, but all other compounds have been structurally characterised.

Solid-state structures

$[Li(O{=}PPh_3)(MeCN)_2]_2[UO_2Cl_4]\cdot MeCN$. The solid state structure of **2** is shown in Fig. 1. The bond lengths within the uranyl fragment are as expected based upon structurally characterised examples in the literature (U=O = 1.7730(14) Å, U–Cl = 2.6721(12) and 2.6762(9) Å),[15] whilst the $[Li(O{=}PPh_3)(solv)_2]_2$ fragment, although quite rare, is also unremarkable with Li–O bonds of 1.922(4) and 1.945(4) Å and P=O bonds of 1.5106(14) Å; the average distances are 1.984 Å and 1.512 Å respectively.[16] The supramolecular structure consists of layers of $[UO_2Cl_4]^{2-}$ anions and $[Li(O{=}PPh_3)(MeCN)_2]_2$ cations held together by extensive C–H···O hydrogen bonds[17] between the U=O and the acetonitrile (2.676 Å) or phenyl (2.575 and 2.452 Å) groups, and C–H···Cl hydrogen bonds between the acetonitrile of the anionic unit (2.937 and 2.911 Å) and phenyl groups (2.937 and 2.911 Å). Notably these C–H···Cl interactions are bifurcated hydrogen bonds, which are common in uranyl halide/pyridinium structures,[18] and in imidazolium type ionic liquids.[19] There are no π–π interactions between the aryl rings. The acetonitrile solvent molecules seemingly aid the assembly of this species.

$[UO_2Br_2(O{=}PPh_3)_2]$. **3** has been prepared previously,[20] but the solid-state structure has not been reported; this is shown in Fig. 2. The uranium metal centre is six coordinate, with bromide and triphenylphosphine oxide ligands lying in a mutually *trans* positions about the uranium centre. The U=O bond length is 1.7511(3) Å and the U–Br bond length of 2.8373(7) Å is slightly longer than the U–Cl bond in $[UO_2Cl_2(O{=}PPh_3)_2]$, (2.645(5) Å) but similar to the U–Br bond in $[UO_2Br_2(O{=}AsPh_3)_2]$ (2.828(1) Å).[21] In the bis imido analogue, $[U(=N^tBu)_2Br_2(O{=}PPh_3)_2]$ the U–Br bond length is slightly longer at 2.8677(14) Å.[11] The U–O and P=O bond lengths of 2.3066(4) Å and 1.522(4) Å is essentially identical to that seen in $[UO_2Cl_2(O{=}PPh_3)_2]$. The supramolecular structure consists of layers of $[UO_2Br_2(O{=}PPh_3)_2]$ held together by π–π interactions and C–H···O hydrogen bonds between the uranyl oxygen and the phenyl rings (2.587 Å). Bifurcated C–H···Br hydrogen bonds are also found (3.103, 3.155 Å),[17] as observed in $[C_6mim]_2[UO_2Br_4]$ (C_6mim = 1-hexyl-3-methylimidazolium).[6e]

$[Li(O{=}PPh_3)_4][I_3]$. The structure of **5** is shown in Fig. 3. It consists of layers of $[Li(O{=}PPh_3)_4]$ cations and I_3 anions. The lithium centre is tetrahedrally coordinated by four $O{=}PPh_3$ molecules each. The average distance for P=O bonds is 1.487 Å and for Li–O is 1.879 Å, similar to those observed for $[Li(O{=}PPh_3)(MeCN)_2]_2[UO_2Cl_4]$. The I–I–I bond is linear with bond lengths of 2.9204(5) and 2.9094(5) Å.

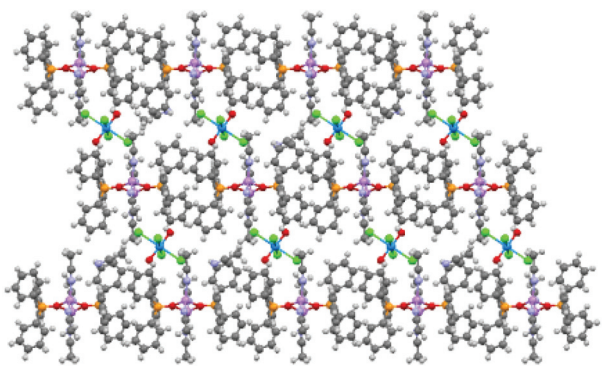

Fig. 1 Packing diagram of $[Li(O{=}PPh_3)(MeCN)_2]_2[UO_2Cl_4]$, **2**.

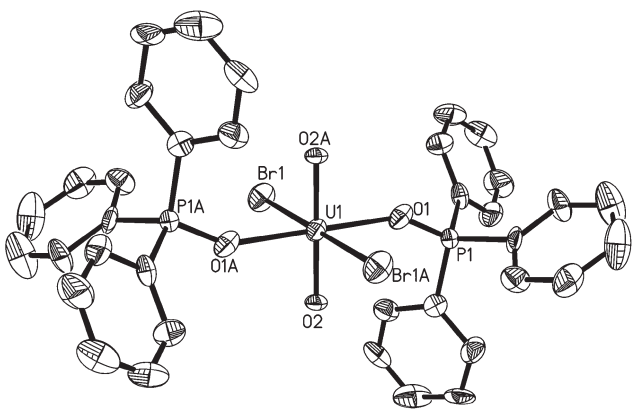

Fig. 2 ORTEP diagram of the solid-state structure of $[UO_2Br_2(O{=}PPh_3)_2]$, **3**. Ellipsoids are shown with 50% probability. Hydrogen atoms are omitted for clarity.

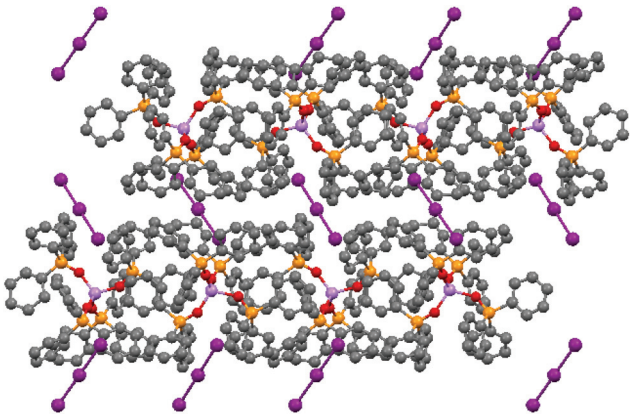

Fig. 3 Supramolecular structure of $[Li(O{=}PPh_3)_4][I_3]$, **5**.

Spectroscopic characterisation

$^{31}P\{^1H\}$ NMR spectroscopy confirms the structural formulation with the phosphine oxide coordinated to the uranium appearing as a singlet at 28 and 31 ppm for **3** and **4** respectively which matches the literature values (Fig. 4), whilst the phosphine oxide coordinated to the Li centre in **2** appear at lower fields (*ca.* 50 ppm). The uranyl moiety has pronounced vibrational modes that are active in both the IR (ν_3 asymmetric) and Raman (ν_1 symmetric) spectra. For **1** these bands are observed at 915 and 839 cm^{-1}, for **2** at 928 and 847 cm^{-1} and for **3** at 920 and 839 cm^{-1} (Fig. S1 and S2†). In addition the P═O stretching frequencies for **3** and **4** are found at 1052 cm^{-1}, identical to that found in **1**.

The electronic absorption spectra of pure (by $^{31}P\{^1H\}$ NMR spectroscopic analysis) solutions of **1**, **3** and **4** in MeCN display three features: an intense band centred at λ_{max} = 230 nm assigned to a spin allowed π–π* transition within the phenyl chromophore (Fig. S3†); a broad, featureless ligand-to-metal charge transfer (LMCT) transition from the equatorial bound halide to the uranium cation at *ca.* λ_{max} = 300 nm for complex **1** which displays a bathochromic shift to 325 nm and 350 nm for **3**, and **4** respectively (Fig. 5); and weak transition centred at

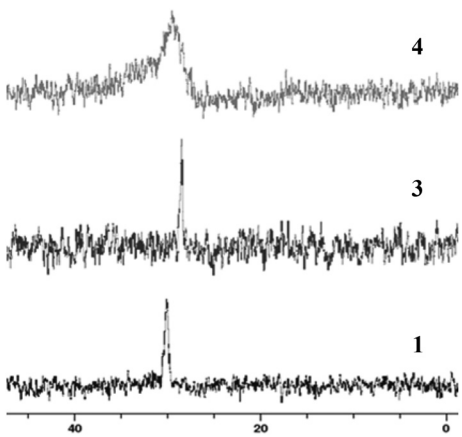

Fig. 4 $^{31}P\{^1H\}$ NMR spectra of **1**, **3** and **4** at 298 K in CD_3CN.

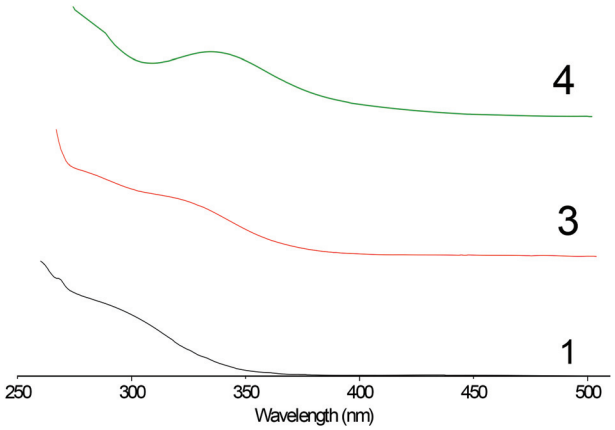

Fig. 5 U–X LMCT region of the electronic absorption spectra of **1**, **3** and **4** in MeCN.

ca. 450–500 nm characteristic of the Laporte forbidden O_{yl}→U LMCT transition with an extinction coefficient of ε = 50 M cm^{-1} for all samples (Fig. S4†). The observed red shift for the charge transfer transition resulting from the halide-to-uranium LMCT compares reasonably well with the reported theoretical values for the halide to uranyl charge transfer in $[UO_2X_4]^{2-}$.[22]

Emission spectroscopy of the actinides has become an important technique for characterisation of the electronic structure,[23] although emission spectra of uranyl in non-aqueous media have lagged behind that of uranyl compounds in aqueous media.[24] **1**, **3** and **4** allow an opportunity to explore the influences of the halide on the photophysical properties of the uranyl ion, although it should be noted that **1** has previously been reported.[24] Also included in our study is the anionic species $[PyH]_2[UO_2Cl_4]\cdot 2Py$. Excitation into either of the absorption bands (between 230 and 460 nm) produces photoluminescence spectra dominated by the corresponding O_{yl}→U LMCT emission bands at *ca.* 515 nm to 520 nm. Pertinent values are recorded in Table 1 and the excitation and emission spectra are shown in Fig. 6. As seen in previously reported examples,[24] only the U–X and U═O LMCT bands are observed in the excitation spectra, suggesting that, in direct contrast to lanthanide emission spectroscopy, the ligand π→π* is not sensitising the emission. It is worth noting that $[UO_2Br_4]^{2-}$ ions have been reported to be weakly emissive with various pyridinium cations.[6c]

Table 1 Photochemical properties of **1**, **3**, **4** and $[PyH]_2[UO_2Cl_4]\cdot 2Py$ in MeCN

Compound	U–X CT (nm)	U═O CT (nm)	λ_{em} (nm)	E_{0-0} (cm^{-1})	τ (μs)	χ^2
1	300	440	515	20 325	1.08	1.07
3	325	445	520	19 267	1.04	1.18
4	350	445	517	20 920	1.04	1.78
1[a]	300	428	529	19 860	1.04	1.00
$[PyH]_2[UO_2Cl_4]\cdot 2Py$	300	430	509	20 661	0.12	1.62

[a] In DCM from ref. 24.

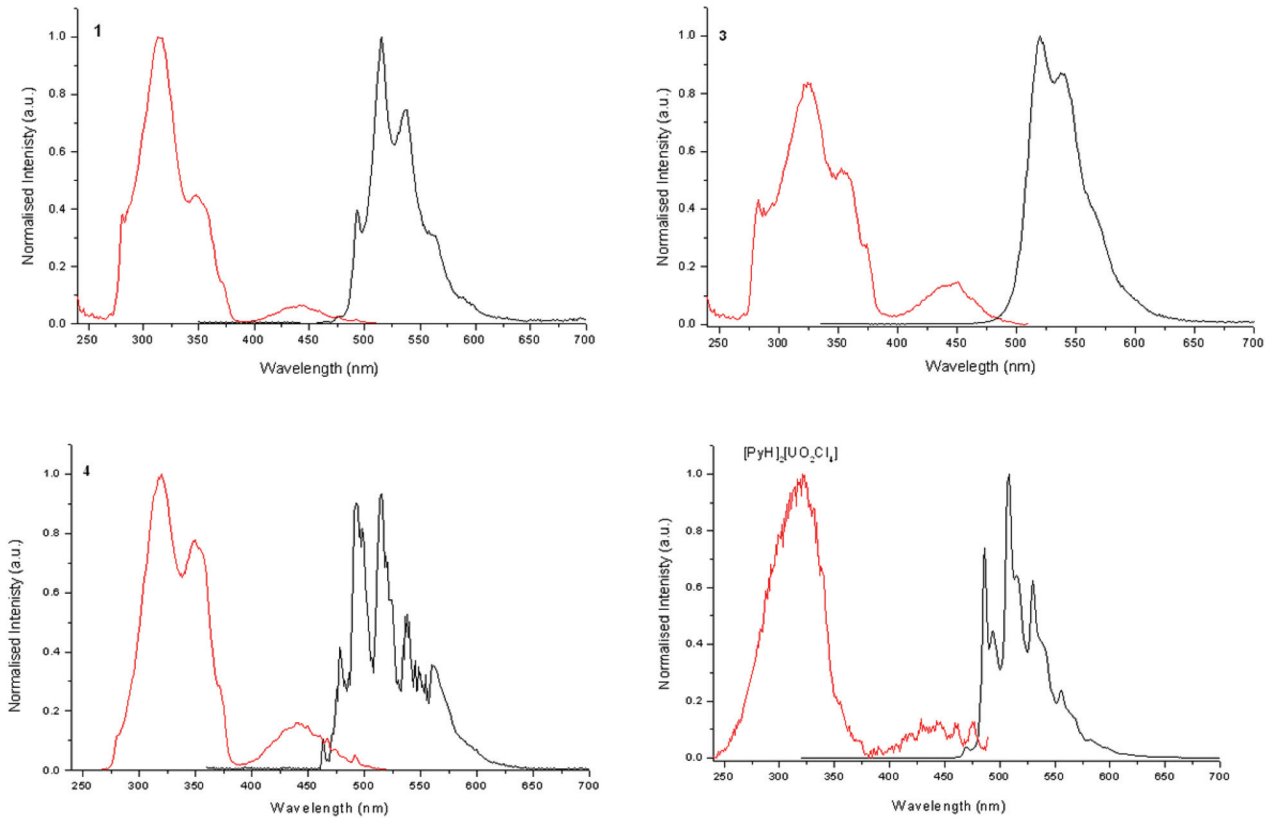

Fig. 6 Excitation (red) and emission (black) spectra of **1**, **3**, **4** and $[PyH]_2[UO_2Cl_4]\cdot 2Py$ in MeCN at 298 K (λ_{ex} = 230–350 nm, λ_{em} = 520 nm).

As seen from Fig. 6, the maxima of the emission spectra for complexes **1**, **3**, **4** and $[PyH]_2[UO_2Cl_4]\cdot 2Py$ are almost identical and no red shift matching that reported for complexes where the donor ligand was changed. For example, in the *trans*-$[UO_2Cl_2L_2]$ system, a red shift in the $O_{yl}\rightarrow U$ LMCT band in line with the increased donor strength was observed and a shift from 517 nm to 529 nm to 531 nm for L = $Ph_3P{=}NH$, $Ph_3P{=}O$ and $Ph_3As{=}O$ respectively was reported in DCM. This observed red shift was postulated to signify a decrease in uranyl oxo bond order as a consequence of increased electron donation from the ancillary ligand in the equatorial plane to the uranium centre. Interestingly, for complexes **1**, **3** and **4**, the only difference observed is the small shift in the halide-to-uranium charge transfer transition in the absorption profile from 300 nm to 325 nm to 350 nm for Cl, Br and I respectively, in line with the increase in bond length. Notably, the emission maximum for **1** in MeCN is different to that reported in DCM (520 nm), so solvation effects are also important in determining the position of the emission bands.

The fine vibrationally resolved structure of the $O_{yl}\rightarrow U$ LMCT band is an indication that non-radiative back energy transfer quenching mechanisms to the aromatic electronic excited levels have been eliminated. The spectrum of **4** is particularly well resolved and the vibronic progression that correspond to the ν_1 and ν_2 vibrational modes (828 cm^{-1}) match reasonably well with that determined from the Raman spectra (839 cm^{-1}). Similarly for **1**, the vibronic progression is 833 cm^{-1} matching previous reports.[24] The luminescence lifetime of all complexes were determined by the correlated single photon counting on nanosecond scale for $[PyH]_2[UO_2Cl_4]$ and microsecond scale for complexes **1**, **3** and **4** following excitation at 294 nm with a nanoLED (Table 1). The kinetic decay profile of all complexes was fitted to a mono-exponential decay. The luminescence lifetimes for $[PyH]_2[UO_2Cl_4]$ in MeCN was measured to be 120 ns whilst the luminescence life times for **1**, **3** and **4** were measured to be *ca.* 1 μs (*cf.* τ = 1.0 μs for $[UO_2(NO_3)_2]\cdot 6H_2O$ in H_2O). No significant change in lifetime was observed for the different halide system in **1**, **3** and **4**, in line with the fact that photoinduced electron transfer (PET) is the main quenching mechanism in uranyl halides.[25] Consistent with this is when the number of halides is increased in $[PyH]_2[UO_2Cl_4]\cdot 2Py$ the lifetime is dramatically reduced. This lifetime is much shorter than that measured for $[UO_2Cl_4]^{2-}$ anions with different cations (for example $MeBu_3N$ in the ionic liquid $MeBu_3N[Tf_2N]$ τ = 0.7 μs)[26] so further mechanisms that increase the non-radiative deactivation of the excited state must occur in this system. The crystal structure of $[PyH]_2[UO_2Cl_4]\cdot 2Py$ has been reported by us[13a] and shows extensive C–H···Cl, C–H···O and C–H···N hydrogen bonding. We therefore tentatively ascribe the short lifetime to a quenching mechanism by exchange of the solvated pyridine molecules.

Conclusions

The oxidation of $[UX_5(THF)]^-$ in the presence of $Ph_3P{=}O$ affords different products depending upon the halide, and these have been structurally characterised. For $[Li(O{=}PPh_3)(MeCN)]_2[UO_2Cl_4]$, C–H···Cl hydrogen bonding is present, and in the species $[UO_2Br_2(O{=}PPh_3)_2]$ long C–H···Br hydrogen bonds are observed. The isolation of $[UO_2X_2(O{=}PPh_3)_2]$ (X = Cl, Br, I) has allowed a comparison of the photophysical properties of the uranyl ion where the halide is systematically changed. The LMCT band originating from the halide shows a bathochromic shift, but the emission maxima and lifetimes of the $O_{yl}{\rightarrow}U$ LMCT band are not particularly sensitive to variation of the halide.

Experimental section

Caution! Natural uranium was used during the course of these experiments. As well as the radiological hazards, uranium is a toxic metal and care should be taken with all manipulations.

All manipulations were carried out using standard Schlenk and glove box techniques under an atmosphere of high purity argon. ^1H, $^{13}C\{^1H\}$ and $^{31}P\{^1H\}$ NMR spectra were recorded on a Bruker AV400 spectrometer operating at 400.23 MHz, 155.54 MHz and 162 MHz respectively, and were referenced to the residual ^1H resonances of the solvent used or external H_3PO_4. IR spectra were recorded on a Perkin Elmer Spectrum One spectrometer with attenuated total reflectance (ATR) accessory. Raman spectra were obtained using 785 nm excitation on a Renishaw 1000 micro-Raman system in sealed capillaries. X-ray crystallography was measured on either a Rikagu Saturn or Bruker Apex Duo diffractometer. The structures were solved by direct methods and refined on F^2 by full matrix least squares (SHELX97)[27] using all unique data. Crystal data, details of data collections and refinement are given in Table 2. CCDC 959953–959955 contains the supplementary crystallographic data for this paper. UV-vis/NIR measurements were made on a Perkin Elmer Lambda 1050 spectrometer using fused silica cells with a path length of 1 cm. Emission spectra were recorded on a Horiba–Jobin–Yvon Fluorolog-3 spectrometer. THF was distilled over potassium, acetonitrile and d_3-acetone were distilled over CaH_2 and degassed immediately prior to use. Spectroscopic measurements used spectroscopic grade solvents which were purchased from commercial sources and dried over molecular sieves and thoroughly degassed before use. $[Li(THF)_4][UX_5(THF)_3]$ (X = Cl, Br, I) were made *via* the literature procedure whilst all other reagents were obtained from commercial sources and dried appropriately.

$[Li(Ph_3PO)(MeCN)]_2[UO_2Cl_4]$

To a solution of $[Li(THF)_4][UCl_5(THF)]$ (0.10 g, 0.129 mmol) in THF was added two equivalents of triphenylphosphine oxide (72 mg, 0.257 mmol) in THF (10 cm^3) and this was stirred for 24 hours at room temperature. The resulting yellow solution was filtered and the solvent was removed under high vacuum. Dissolution in acetonitrile and placement at −30 °C overnight yielded clear yellow crystals of **1** (0.056 g, 48%) whose NMR and infrared data are in accord with the literature. Concentration of the mother liquor and placement at −30 °C overnight yielded yellow crystals of **2** (0.02 g 11%). ^1H NMR (CD_3CN, 298 K): 7.55–7.67 (m, Ph); ^{31}P NMR (CD_3CN, 298 K): 48.51 ppm (s, Li–O=PPh_3); IR (cm^{-1}): 1439, 1120, 1060, 1025, 995, 919 (U=O), 764, 753, 726, 690; Raman (cm^{-1}): 1589, 1572, 1487, 1440, 1190, 1164, 1137, 1088, 1028, 1000, 929, 839 (O=U), 727, 687, 617, 417, 301. 256, 207, 193.

$[UO_2Br_2(O{=}PPh_3)_2]$

To a solution of $[Li(THF)_4][UBr_5(THF)]$ (0.10 g, 0.10 mmol) in THF was added two equivalents of triphenylphosphine oxide

Table 2 Crystallographic data and structure refinement for complexes **2**, **3** and **5**

	2	**3**	**5**
Empirical formula	$C_{48}H_{48}Cl_4Li_2N_6O_4P_2U$	$C_{36}H_{30}Br_2O_4P_2U$	$C_{72}H_{60}I_3LiO_4P_4$
FW (g mol^{-1})	1228.57	986.39	1500.72
Crystal system	Triclinic	Monoclinic	Monoclinic
Space group	$P\bar{1}$	$P21/c$	$P21/c$
Temperature (K)	108(2)	170(2)	103(2)
a (Å)	9.5374(19)	9.2695(19)	16.4991(9)
b (Å)	12.329(3)	10.430(2)	23.6236(12)
c (Å)	13.578(3)	18.221(4)	23.0801(9)
α (°)	114.91(3)	90.00	90.00
β (°)	93.92(3)	97.91(3)	132.690(2)
γ (°)	108.10(3)	90.00	90.00
V (Å^3)	1339.2(5)	1744.9(6)	6612.3(6)
σ_{calcd} (Mg m^{-3})	1.523	1.877	1.508
M (mm^{-1})	3.335	7.070	1.562
F(000)	606	940	2984
Collected reflections	12 900	17 097	103 271
Independent reflections	6805	3022	15 824
R_{int}	0.0184	0.1519	0.0527
R_1 [$I > 2\sigma(I)$]	0.0193	0.1019	0.0422
wR_2 [all data]	0.0560	0.2991	0.0967
Goodness of fit on F^2	1.081	1.149	1.030

(55.66 mg, 0.2 mmol) in THF (10 cm^3) and this was stirred for 24 hours at room temperature. The resulting yellow solution was filtered and the solvent was removed under high vacuum. Dissolution in acetonitrile and placement at −30 °C overnight yielded dark yellow crystals suitable for X-ray diffraction (41 mg, 41.6%). ^{1}H NMR (CD_3CN, 298 K): 7.67–7.57 ppm (m, Ph); ^{31}P NMR (CD_3CN, 298 K): 28.46 ppm; IR (cm^{-1}): 1439, 1120, 1050, 1025, 995, 928 (U═O), 764, 753, 726, 690; Raman (cm^{-1}): 1590, 1672, 1487, 1440, 1190, 1164, 1137, 1088, 1028, 1000, 929, 847 (U═O), 727, 687, 617, 417, 301. 256, 207, 193.

$[UO_2I_2(O{=}PPh_3)_2]$

To a solution of $[Li(THF)_4][UCl_5(THF)]$ (100 mg, 0.129 mmol) in THF (5 cm^3) was added Me_3SiI in excess. The solution was stirred for 24 hours to give a pale yellow solution. The solvent was removed under vacuum and the remaining orange powder was dissolved in acetonitrile (10 cm^3). To this was added 2 equivalents of $O{=}PPh_3$ (72 mg, 0.257 mmol) in MeCN (5 cm^3) and the reaction was stirred for a further 24 hours. The resulting orange solution was filtered and the solvent was reduced in volume. Placement at −30 °C overnight yielded dark orange crystals of **4** and orange powder of **5** (19 mg, 0.018 mmol, 13.6%) which were separated by hand. Spectroscopic data for **4** were in accord with the literature data. ^{1}H NMR (400 MHz, CD_3CN, 298 K): δH = 7.55–7.69 (m, Ar–H) ppm; ^{31}P NMR (400 MHz, CD_3CN, 298 K): 31.2 ppm (s, U–O═PPh_3); IR (cm^{-1}): 1439 (s), 1120 (m), 1052 (s, P═O), 1025 (m), 995 (m, O═U), 920 (m), 764 (m), 753 (m), 726 (s), 690 (s); Raman (cm^{-1}): 1590 (w), 1568 (w), 1265 (w), 1229 (m), 1185 (m), 1156 (w), 1137 (w), 1090 (w), 1028 (w), 1000 (s), 839 (s, O═U), 687 (m), 617 (m). Anal. Calcd for $C_{36}H_{30}O_4P_2I_2U$: C, 40.02; H, 2.79%. Found: C, 38.83; H, 2.07.

Acknowledgements

We thank TCD for funding this work.

Notes and references

1 For leading references see: (*a*) V. Mougel, C. Camp, J. Pécaut, C. Copéret, L. Maron, C. E. Kefalidis and M. Mazzanti, *Angew. Chem., Int. Ed.*, 2012, **51**, 12280; (*b*) A.-C. Schmidt, A. V. Nizovtsev, A. Scheurer, F. W. Heinemann and K. Meyer, *Chem. Commun.*, 2012, **48**, 8634; (*c*) D. M. King, F. Tuna, E. J. L. McInnes, J. McMaster, W. Lewis, A. J. Blake and S. T. Liddle, *Science*, 2012, **337**, 717; (*d*) B. M. Gardner, J. C. Stewart, A. L. Davis, J. McMaster, W. Lewis, A. J. Blake and S. T. Liddle, *Proc. Natl. Acad. Sci. U. S. A.*, 2012, **109**, 9265; (*e*) O. P. Lamb and K. Meyer, *Polyhedron*, 2012, **32**, 1; (*f*) O. P. Lam, F. W. Heinemann and K. Meyer, *Chem. Sci.*, 2011, **2**, 1538; (*g*) P. L. Arnold, *Chem. Commun.*, 2011, **47**, 9005; (*h*) O. T. Summerscales and F. G. N. Cloke, *Struct. Bonding*, 2008, **127**, 87; (*i*) O. P. Lam, C. Anthon and K. Meyer, *Dalton Trans.*, 2009, 9677; (*j*) A. J. Lewis, P. J. Carroll and E. J. Schelter, *J. Am. Chem. Soc.*, 2013, **135**, 511.

2 For recent reviews see: (*a*) M. B. Jones and A. J. Gaunt, *Chem. Rev.*, 2013, **113**, 1137; (*b*) R. J. Baker, *Coord. Chem. Rev.*, 2012, **256**, 2843; (*c*) T. W. Hayton, *Dalton Trans.*, 2010, **39**, 1145; (*d*) S. T. Liddle and D. P. Mills, *Dalton Trans.*, 2009, 5592; (*e*) S. T. Liddle, *Proc. R. Soc. London, Ser. A*, 2009, **465**, 1673; (*f*) I. Castro-Rodríguez and K. Meyer, *Chem. Commun.*, 2006, 1353; (*g*) M. Ephritikhine, *Dalton Trans.*, 2006, 2501.

3 (*a*) M. L. Neidig, D. L. Clark and R. L. Martin, *Coord. Chem. Rev.*, 2013, **257**, 394; (*b*) N. Kaltsoyannis, *Inorg. Chem.*, 2013, **52**, 3407.

4 R. J. Baker, *Chem.–Eur. J.*, 2012, **18**, 16258.

5 R. G. Denning, *J. Phys. Chem. A*, 2007, **111**, 4125.

6 (*a*) M. B. Andrews and C. L. Cahill, *Dalton Trans.*, 2012, **41**, 911; (*b*) R. E. Wilson, S. Skanthakumar, C. L. Cahill and L. Soderholm, *Inorg. Chem.*, 2011, **50**, 10748; (*c*) N. P. Deifel and C. L. Cahill, *C. R. Chim.*, 2010, **13**, 747; (*d*) M.-O. Sornein, M. Mendes, C. Cannes, C. Le Naour, P. Nockemann, K. Van Hecke, L. Van Meervelt, J.-C. Berthet and C. Hennig, *Polyhedron*, 2009, **28**, 1281; (*e*) P. Nockemann, K. Servaes, R. Van Deun, K. Van Hecke, L. Van Meervelt, K. Binnemans and C. Goerller-Walrand, *Inorg. Chem.*, 2007, **46**, 11335; (*f*) R. Bohrer, E. Conradi and U. Mueller, *Z. Anorg. Allg. Chem.*, 1988, **558**, 119; (*g*) G. Van den Bossche, M. R. Spirlet, J. Rebizant and J. Goffart, *Acta Crystallogr., Sect. C: Cryst. Struct. Commun.*, 1987, **43**, 383; (*h*) E. Conradi, R. Bohrer and U. Mueller, *Chem. Ber.*, 1986, **119**, 2582; (*i*) L. Di Sipio, E. Tondello, G. Pelizzi, G. Ingletto and A. Montenero, *Cryst. Struct. Commun.*, 1977, **6**, 723; (*j*) L. Di Sipio, E. Tondello, G. Pelizzi, G. Ingletto and A. Montenero, *Cryst. Struct. Commun.*, 1974, **3**, 301; (*k*) L. Di Sipio, E. Tondello, G. Pelizzi, G. Ingletto and A. Montenero, *Cryst. Struct. Commun.*, 1974, **3**, 297; (*l*) Y. N. Mikhailov and V. G. Kuznetsov, *Zh. Neorg. Khim.*, 1971, **16**, 2512; (*m*) Y. N. Mikhailov, V. G. Kuznetsov and E. S. Kovaleva, *Zh. Neorg. Khim.*, 1965, **6**, 787.

7 M.-J. Crawford, A. Ellern, K. Karaghiosoff, P. Mayer, H. Nöth and M. Suter, *Inorg. Chem.*, 2004, **43**, 7120.

8 M.-J. Crawford, A. Ellern, H. Nöth and M. Suter, *J. Am. Chem. Soc.*, 2003, **125**, 11778.

9 J.-C. Berthet, M. Nierlich and M. Ephritikhine, *Chem. Commun.*, 2004, 870.

10 M.-J. Crawford and P. Mayer, *Inorg. Chem.*, 2005, **44**, 5547.

11 L. P. Spencer, P. Yang, B. L. Scott, E. R. Batista and J. M. Boncella, *C. R. Chim.*, 2010, **13**, 758.

12 (*a*) R. J. Baker and A. Walshe, *Chem. Commun.*, 2012, **48**, 985; (*b*) J. Fang, A. Walshe, L. Maron and R. J. Baker, *Inorg. Chem.*, 2012, **51**, 9132; (*c*) A. Walshe, J. Fang, L. Maron and R. J. Baker, *Inorg. Chem.*, 2013, **52**, 9077.

13 (*a*) E. Hashem, A. N. Swinburne, C. Schulzke, R. C. Evans, J. A. Platts, A. Kerridge, L. S. Natrajan and R. J. Baker, *RSC Adv.*, 2013, **3**, 4350; (*b*) E. Hashem, G. Lorusso, M. Evangelisti, T. McCabe, C. Schulzke, J. A. Platts and R. J. Baker, *Dalton Trans.*, 2013, **42**, 14677.

14 G. Bombieri, E. Forsellini, P. J. Day and W. I. Azeez, *J. Chem. Soc., Dalton Trans.*, 1978, 677.
15 (*a*) D. J. Watkin, R. G. Denning and K. Prout, *Acta Crystallogr., Sect. C: Cryst. Struct. Commun.*, 1991, **47**, 2517; (*b*) R. J. Baker, E. Hashem, M. Motevalli, H. V. Ogilvie and A. Walshe, *Z. Anorg. Allg. Chem.*, 2010, **636**, 443.
16 Determined from a survey of the Cambridge Structural Database.
17 The most recent IUPAC definition of a hydrogen bond states that "*in most cases, the distance between H and Y are found to be less than the sum of their van der Waals radii*": E. Arunan, G. R. Desiraju, R. A. Klein, J. Sadlej, S. Scheiner, I. Alkorta, D. C. Clary, R. H. Crabtree, J. J. Dannenberg, P. Hobza, H. G. Kjaergaard, A. C. Legon, B. Mennucci and D. Nesbitt, *Pure Appl. Chem.*, 2011, **83**, 1637. According to this criterion, H···Y distances of less than 2.72 Å for a C–H···O, 2.95 Å for C–H···Cl and 3.06 Å for C–H···Br are classed as hydrogen bonds. Van der Waals radii taken from S. Alvarez, *Dalton Trans.*, 2013, **42**, 8617.
18 (*a*) N. P. Deifel and C. L. Cahill, *CrystEngComm*, 2009, **11**, 2739; (*b*) M. B. Andrews and C. L. Cahill, *Dalton Trans.*, 2012, **41**, 3911; (*c*) N. P. Deifel and C. L. Cahill, *C. R. Chim.*, 2010, **13**, 747.
19 M. Deetlefs, C. L. Hussey, T. J. Mohammed, K. R. Seddon, J.-A. van den Berg and J. A. Zora, *Dalton Trans.*, 2006, 2334.
20 J. P. Day and L. M. Venanzi, *J. Chem. Soc. A*, 1966, 1363.
21 F. J. Arnaiz, M. J. Miranda, R. Aguado, J. Mahia and M. A. Maestro, *Polyhedron*, 2000, **20**, 3295.
22 F. Ruiperez and U. Wahlgren, *J. Phys. Chem. A*, 2010, **114**, 3615.
23 L. S. Natrajan, *Coord. Chem. Rev.*, 2012, **256**, 1583.
24 M. P. Redmond, S. M. Cornet, S. D. Woodall, D. Whittaker, D. Collison, M. Helliwell and L. S. Natrajan, *Dalton Trans.*, 2011, **40**, 3914.
25 Z. Fazekas, T. Yamamura and H. Tomiyasu, *J. Alloys Compd.*, 1998, **271–273**, 756.
26 M.-O. Sornein, C. Cannes, C. Le Naour, G. Lagarde, E. Simoni and J.-C. Berthet, *Inorg. Chem.*, 2006, **45**, 10419.
27 G. M. Sheldrick, *SHELXL-97*, University of Göttingen, Göttingen, Germany, 1998.